Thermodynamic Processes in the Lakes on the Thermal Bar Development under Condition of the Coriolis Effect

N. S. Blokhina[a], D. A. Solov'ev[b]

[a] Moscow State University, Moscow, 119992 Russia
[b] P.P. Shirshov Institute of Oceanology, Russian Academy of Sciences, 36 Nakhimovskii ave., Moscow, 117997 Russia,
e-mail: blokhina@phys.msu.ru, solovev@sail.msk.ru

Abstract—In this work, a mathematical model of a springtime thermal bar is constructed. A closed system of Reynolds-type equations is used; it is constructed based on a nonlinear system of thermohydrodynamic equations with the use of a special method for extracting the large-scale structures in a turbulent medium. A numerical solution of this system in a water reservoir with an inclined bottom is obtained; the contribution introduced by the Coriolis force into thermodynamic processes in a water reservoir in the period of existence of a springtime thermal bar is demonstrated.

Key words: mathematical simulation, Coriolis effect, thermal bar, convection, turbulence, field observations

DOI: 10.3103/S0027134910030094

INTRODUCTION

In late winter the water temperature in many mid-latitude lakes is less than 4°C, i.e., the temperature at which the density of fresh water reaches its maximum value. Because of the surface waters reach the temperature of the maximum density near the coast faster, in water reservoirs a horizontal pressure gradient appears, which leads to the formation of two circulation cells with a convergence zone near surface waters with a temperature of about 4°C (Fig. 1). This zone, extending from surface to bottom, is conventionally called a thermal bar. Thermal bar inhibit horizontal water mixing between two circulation cells and the penetration of coastal pollutants to the central part of a water reservoir. As a water reservoir is heated, the thermal bar migrates from the coastal part of the water reservoir to its center and disappears after the temperature of the entire water reservoir becomes greater than 4°C. This phenomenon can also be observed during the fall when the surface waters cool to the temperature of 4°C. We note that in large lakes, where the thermal bar exists for a few months, the phenomenon associated with the action of the Coriolis force becomes important; this phenomenon may have an appreciable effect on the dynamics of the liquid motion in water reservoirs and, hence, on the appearance and development of a thermal bar.

For the horizontal scale L of a water reservoir, the effect of the Earth's rotation can be neglected, whereas the time required to move a liquid particle a distance L is much less than the period of the Earth's rotation. Thus, it can be conjectured that the effect of the Coriolis force will be significant for: $L/V \gg \Omega^{-1}$, where Ω is the angular speed of the Earth's rotation, and V is the average speed of the convective flows. This condition is equivalent to the relation $V/\Omega L \ll 1$, which is conventionally called the Rossby−Obukhov number (Ro). It is easily shown that the minimum horizontal scale L of the water reservoir, whose pattern of the convective flows will be markedly affected by the Earth's rotation, may be 1.5 km or larger.

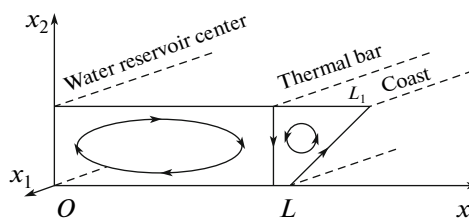Since the thermal bar phenomenon was discovered by Forel in Lake Geneva in 1880, more than 60 years

Fig. 1. Scheme of the modeled water reservoir with indication of the direction of motion of flow lines and position of the thermal bar in initial phase of its development. H is the depth of the water reservoir, L is the reservoir width at the bottom, and L_1 is the reservoir width at the surface.

elapsed before systematic studies of this phenomenon were initiated. First of all, these were the field observations in Yakimansk bay of Ladoga Lake that were initiated by A.I. Tikhomirov [2, 3] and continued subsequently by both Russian and foreign researchers in the Onega, Ladoga, and Great lakes, as well as other lakes of the world [4–6]. Those works present the data on the distribution of the fields of the temperatures and flow speeds in the thermal frontal zone and speeds of thermal bar motion. The data of many authors suggest that the speed of thermal bar propagation may range from 200 to 1000 meters per day. It was found that the horizontal components of flow speed in the vicinity of a front are close to 0.01–0.05 m/s. Based on analysis of a multiyear observation database, researchers have derived empirical dependence relating the lake depth *H* overlain by the 4°C isotherm on the water surface to the observation dates. This empirical formula made it possible to determine the average position of the springtime thermal frontal zone on the surface of Ladoga Lake for any date [6]. Formulas were derived to calculate the propagation speed of the thermal bar, taking into account the vertical heat flow into the water surface [7] and the heating effect of the warm coastal zone [8]. However, all works dealing with these field observations have disregarded the specific features of the currents caused by the Coriolis force. This issue is also omitted in studies concerned with laboratory simulation of thermal bar, due to size limitations on the laboratory setup. Only theoretical studies can indicate the specific features of the currents by taking the Coriolis force in hydrodynamic equations into account.

All earlier theoretical studies of the thermal bar phenomenon can be split into two categories. Studies of the first category concentrate on prediction of the propagation of thermal bar; they are based on heat balance models [2, 9, 10], again disregarding the specific features of the geostrophic effects. The second category covers the area of mathematical simulations. These studies may provide detailed distribution fields of temperature and flow speeds in water reservoirs of different sizes, with and without taking the Coriolis forces in thermohydrodynamic equations into account; they may also compare the modeling results. Among the most familiar works that have taken the geostrophic effects in momentum transfer equations into account, we can mention [10, 11, 12, and 13]. However, these works focused on the analysis of flows observed in finite areas of water reservoirs near thermal bar. They do not consider the influence of the Coriolis force on the flows in water reservoir for the complete duration of thermal front development and do not perform comparisons with calculations when neglecting geostrophic effects.

The purpose of this work is estimation of the thermohydrodynamic effects in large freshwater reservoirs in the period of occurrences and the total time of the development of a thermal bar using numerical simulation method, when Coriolis force are taken into account in momentum transfer equations.

PROBLEM FORMULATION

This work considers the movement of a liquid in a region that corresponds to half of a water reservoir with a sloping right-hand coast. The region stretches in the x_2 direction and is infinite in the x_1 direction. The problem is solved in the Ox_1, Ox_2, and Ox_3 coordinate system (Fig. 1). The lower left corner is considered as the origin.

To describe the thermohydrodynamic processes in a viscous incompressible liquid, we use a system of Navier–Stokes equations in the Boussinesq approximation, an equation for thermal conductivity, the continuity equation, and the equation of state for freshwater in a temperature region of anomalous density (1):

$$\rho(T) = \rho_0(1 - \gamma(T - 4°C)^2).\tag{1}$$

Here, T is the temperature, ρ and ρ_0 are the water densities at the temperatures T and 4°C respectively, and $\gamma = 0.000085$ deg^{-2}.

It is assumed that the motion along the x_1 axis is uniform and that the large-scale convective structures that occur to the right and to the left of the thermal bar are formed in the turbulent medium. To separate the large-scale structures in the turbulent medium, the system of thermohydrodynamic equations is transformed according to the method suggested in [14]. As a result, we obtain systems of equations for convective ordered structures and the small-scale component of the flow. The system of equations for the small-scale component is not solved. For closure of the first system of equations, we introduce the coefficient of turbulent viscosity ν_T, which is assumed to be constant in the entire study area but variable in time. This coefficient is calculated based on the activity of motion (see equation 6 below). The development of the final system of equations and the equation of closure is presented in [15] in detail. It is noteworthy that we took the fact that the motion along the x_1 axis is uniform into account, which allowed the initial system of equations to be written in variables of the function of current ψ and vorticity φ.

Due to these assumptions, the system of thermohydrodynamic equations and closure equation in dimensionless form are written in the variables ψ, φ, T, and U_1:

$$\frac{\partial U_1}{\partial t} + \frac{\partial \psi}{\partial x_3}\frac{\partial U_1}{\partial x_2} - \frac{\partial \psi}{\partial x_2}\frac{\partial U_1}{\partial x_3} - 2\frac{\partial \psi}{\partial x_3}\Omega\sin\alpha$$
$$= \mu\left(\frac{\partial^2 U_1}{\partial x_2^2} + \frac{\partial^2 U_1}{\partial x_3^2}\right),\tag{2}$$

$$\frac{\partial \varphi}{\partial t} + \left(\frac{\partial \psi}{\partial x_3}\frac{\partial \varphi}{\partial x_2} - \frac{\partial \psi}{\partial x_2}\frac{\partial \varphi}{\partial x_3} \right) + 2\frac{\partial U_1}{\partial x_3}\Omega\sin\alpha$$

$$= \mu\left(\frac{\partial^2 \varphi}{\partial x_2^2} + \frac{\partial^2 \varphi}{\partial x_3^2} \right) - 2(T - T4)\frac{\partial T}{\partial x_2}, \tag{3}$$

$$\frac{\partial T}{\partial t} + \left(\frac{\partial \psi}{\partial x_3}\frac{\partial T}{\partial x_2} - \frac{\partial \psi}{\partial x_2}\frac{\partial T}{\partial x_3} \right) = \mu\left(\frac{\partial^2 T}{\partial x_2^2} + \frac{\partial^2 T}{\partial x_3^2} \right), \tag{4}$$

$$\Delta\psi = \varphi, \tag{5}$$

$$\mu^2 = \left(\frac{\nu_T}{H\sqrt{gH}} \right)^2 = \frac{c^3}{s}\iint_S \left[4\left(\frac{\partial^2 \psi}{\partial x_2 \partial x_3} \right)^2 \right.$$

$$\left. + \left(\frac{\partial^2 \psi}{\partial x_3^2} - \frac{\partial^2 \psi}{\partial x_2^2} \right)^2 \right] ds - (T - T4)\frac{\partial T}{\partial x_3} \right] ds, \tag{6}$$

where U_1 is the speed of water motion along the x_1 coordinate, and α is the geographic latitude. Here, $\mu = \nu_T/H\sqrt{gH}$ is the dimensionless coefficient of turbulent viscosity and $T4$ is the dimensionless temperature of the maximum density of freshwater. In converting the equations in dimensionless form, we choose scales as follows: the depth of the water reservoir H for the distances, $\sqrt{1/\gamma}$ for the temperature, $\sqrt{gH}$ for the speed, and $\sqrt{H/g}$ for the time.

At the upper boundary of the modeled water reservoir ($x_3 = H$), for the speeds we formulated the conditions corresponding to the free boundary for the speed and specified (assumed constant in time and in the area of the water reservoir) the balance radiative heat flux Q that heats the surface waters. At the bottom ($x_3 = 0$) and at the right-hand sloping ($x_2 = LL_1$) lateral boundary of the water reservoir, we specified the conditions for sticking and impermeability for the speed and for the heat flux corresponding to springtime flows obtained from field observations. At the left-hand boundary ($x_2 = 0$) of the region, we specified the symmetry condition for all variables. At the initial time, the liquid in the water reservoir is assumed to be motionless and the temperature at the water surface is assumed to be less than 4°C.

Equations (2)–(5), together with the closure equation (6) and boundary and initial conditions, form a closed system of equations for simulating the dynamics of the convective motion of water masses in a water reservoir in the period of thermal bar development. We considered a water reservoir in the northern hemisphere of Earth at the geographic latitude $\alpha = 60°$. Half of the modeled water reservoir has the length $L_1 = 8880$ m. The maximum depth H of the water reservoir is 150 m. The balance heat flux that arrives at the water surface is $Q = 210$ W/m^2.

To solve the obtained system of equations, we used an implicit absolutely stable finite-difference scheme. The problem was solved with the help of the method of alternating directions on the spatial grid, which consists of 1649 grid points with a dimensionless grid interval in time $\tau = 4$. For the approximation and calculation of the boundary conditions for the functions ψ and φ, we used the approach suggested in [16].

MATHEMATICAL SIMULATION RESULTS

We will describe the dynamics of thermal bar development. Figure 2a presents the fields of distribution of the temperature T and Fig. 2b presents those for the function of current Ψ with the timestep $\Delta t = 7.25$ days. Solids and dashed lines on the figure correspond to the cases when the Coriolis force is taken ($\Omega \neq 0$) and not taken into account ($\Omega = 0$) respectively. Heat influx to the water leads to the fact that the surface waters near the coast attain the temperature for their maximum density (4°C). A frontal interface, namely a thermal bar, starts to form. In this region, warm surface waters descend, simulating downward flow in the narrow band extending from the surface to the bottom of the water reservoir. Simultaneously, in the central part of the water reservoir, the ascent of cold deep waters takes place, which, upon heating, are displaced toward the temperature front with maximum-density waters (Fig. 2, t_1). Thus, the water reservoir becomes separated into two regions, which do not exchange water in the horizontal plane. The front of the thermal bar, which is generally located parallel to the coastal line, gradually migrates to the lake center (Fig. 2, t_1–t_6). The liquid moves counterclockwise in the coastal cell, and it moves clockwise in the deep cell. At the beginning of the water reservoir heating, a deep convective vortex encompasses the entire water reservoir. As far as the surface of the water reservoir warms up, the speed liquid circulation in the deep cell slows down. Simultaneously, the deep cell shrinks, and the coastal cell, on the contrary, grows, replacing the deep circulation. The circulation speed in the coastal cell increases with delivery of heat to the water reservoir surface. The thermal bar disappears (Fig. 2, t_7) when the temperature of the entire area of the water reservoir becomes larger than 4°C. At the same time, the coastal cell occupies the entire region from the right-hand coast to the center of the water reservoir. Analysis of the motion of the thermal bar in the modeled water reservoir showed that 57.3 days elapse from the time of the appearance of the thermal front to its disappearance, and that the average speed of the motion of the 4°C isotherm is 155 m/day. The obtained values qualitatively agree with the data of field observations in different water reservoirs [6, 7, and 10], both for the speed (200–1000 m/day) and the decay time of the thermal bar (1–3 months). From Fig. 2 it is seen that the action of the Coriolis force in the modeled water reservoir leads to marked deceleration of the development process of the thermal bar, which is observed for a few more days. Here, it should be remembered that the
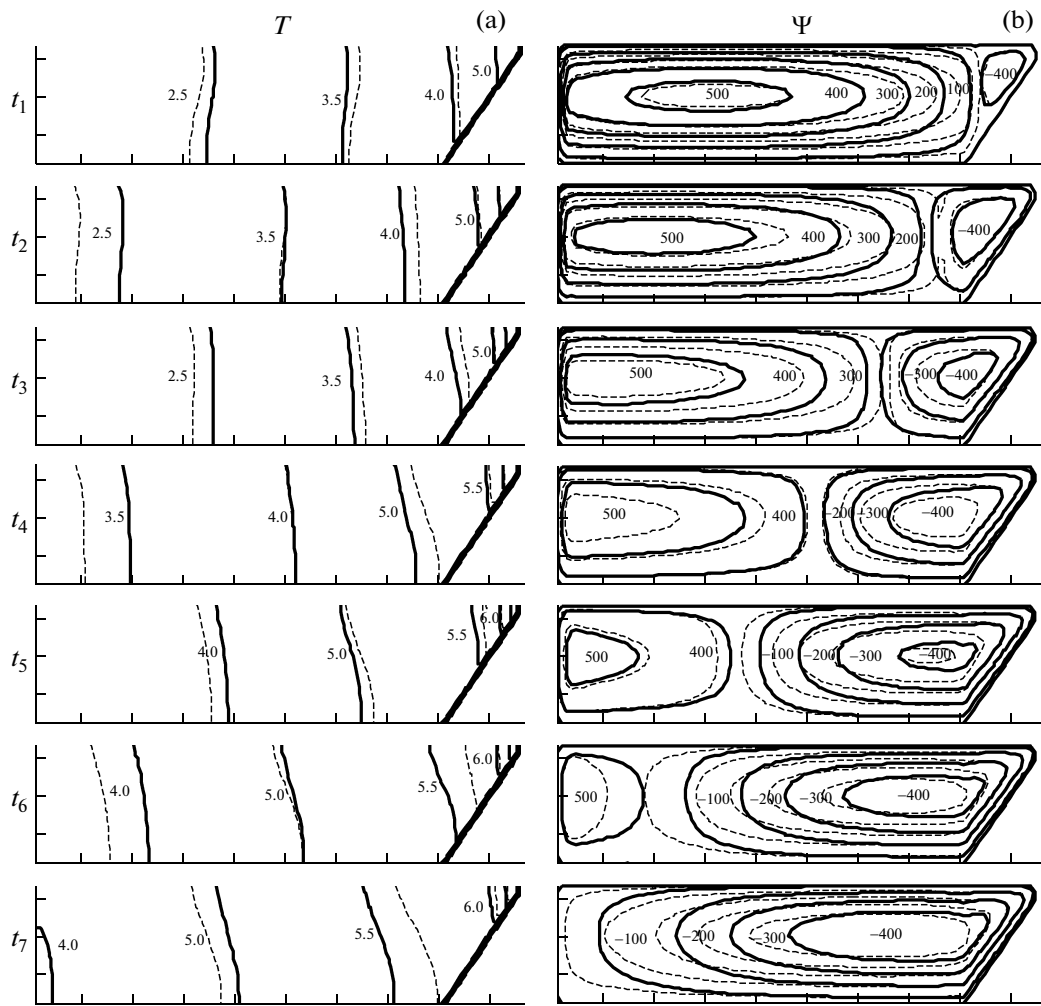
Fig. 2. Fields of distributions of temperature T (a) and and function of current Ψ (b) in the (x_1, x_2) plane with the time step $t =$ 7.25 days. Dashed lines indicate calculations disregarding the Coriolis force ($\Omega = 0$), and solid lines indicate calculations with inclusion of Coriolis force.

water reservoir heating goes all day long, i.e., without taking into account the diurnal variation of thermal balance; therefore, the lifetime of the thermal bar may have been underestimated by a factor of approximately two. The estimate of the average speeds of the liquid motion in the water reservoir within the lifetime of the thermal bar is presented in the Table, which displays the decrease of the average horizontal speed of the liquid circulation U_2 in the water reservoir by approximately 20% ($\Omega \neq 0$).

The mean speeds of liquid motion in a water reservoir within the lifetime of a thermal bar

$U_i \times 10^{-3}$, m/s	$\Omega = 0$	$\Omega \neq 0$
U_1	–	6.5
U_2	1.2	0.9
U_3	13.0	10.0

We will consider the effect of Coriolis force on the speed of propagation of a thermal bar during its motion from the right-hand sloping coast to the center of the water reservoir. The spatial distribution of the circulation speed and direction in the study water reservoir with time step $\Delta t = 14.5$ days (taking into account the Coriolis force) is plotted in Fig. 3. Here, we clearly see how the liquid velocity is deflected to the right from the straight-line motion (in the case when $\Omega = 0$). It is seen that the vector of velocity may be deflected by as much as $10°$ on the water reservoir surface, suggesting that the model water reservoir should have a sufficient size, so that the geostrophic effects can be studied.

At the initial stage of the water reservoir heating, the $4°C$ isotherm, which is indicated by the solid line (Fig. 2, t_1-t_3), shifts faster along the x_2 axis toward the center of the modeled water reservoir than does the $4°C$ isotherm indicated by the dashed line; that is, the speed of the motion of the thermal bar is somewhat
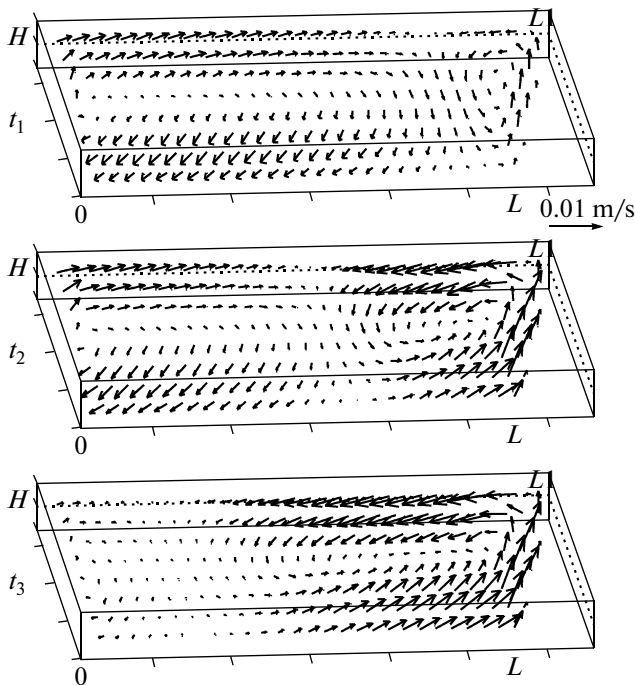
Fig. 3. Fields of the distribution of the water current speed $U(x_1, x_2, x_3)$ in the modeled water reservoir, calculated with the time step $t = 14.5$ days, taking into account the Coriolis force in the hydrodynamic equations.

Fig. 4. Dependence of the Rossby–Obukhov number on the time of the water reservoir heating. Dashed line indicates calculations disregarding the Coriolis force ($\Omega = 0$), and solid lines indicate calculations the with inclusion of the Coriolis force.

larger when the Coriolis force is taken into account. This can be seen from the dependence of the Rossby number (Ro $= V/\Omega L$) on the water reservoir heating time (Fig. 4). Increase of the speed of the thermal bar motion under the influence of the Coriolis force is caused by a decrease of the mean speed of the liquid circulation in the deep circulation cell, which has a large range at the initial stage of the thermal bar formation (Fig. 4). When the thermal bar is in half way to the water reservoir center (Fig. 2, t_4), the cells are close in size and the average speed of the liquid circulation is of the same order of magnitude in both cells (Fig. 4, $t \approx 29$ days). Then, the migration speed of the thermal bar, when the Coriolis force acts, becomes markedly less (Fig. 2, t_5-t_7). This is because the average speed of the liquid circulation is much less in the coastal circulation cell, encompassing the entire modeled water reservoir (Fig. 4).

CONCLUSIONS

Despite considerable simplification, the numerical estimates turned out to be rather close to the data of the field observations [6, 7, 10].

The analysis of the numerical results identified two stages in the general pattern of the convective motions in the water reservoir. Under the impact of the Coriolis force the velocity of the shift of the thermal bar toward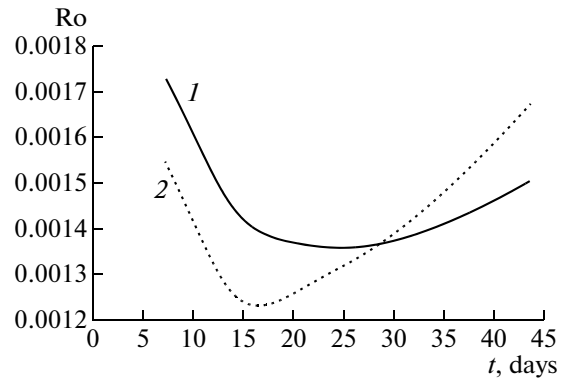s to the water reservoir center is increased at the initial stage of the water reservoir heating, and it is decreased at the final heating stage. Such a character of motion seems to occur because of the differences in the size of the regions with waters that are involved in the convective circulations in deep- and shallow-water regions of the modeled water reservoir at different times.

Inclusion of the Coriolis effect in the mathematical simulation led to the reduction of the mean horizontal speed of the liquid circulation in both circulation cells by approximately 20% and to lengthening of the time of existence of the thermal bar in the water reservoir by approximately 5%.

The obtained results indicate that the geostrophic effects that occur in extended water reservoirs markedly influence the dynamics of the convective flows and on the formation and development of thermal bars This results also indicates that the Coriolis forces should be accounted for in the equations of hydrodynamics during mathematical simulations.

REFERENCES

1. F. A. Forel', *Guide on Lake Research (General Limnology)* (St. Petersburg, 1912) [in Russian].

2. A. I. Tikhomirov, Izv. Vsesoyuz. Geogr. Ob-va **91**, No. 5, 424 (1959).

3. A. I. Tikhomirov, Izv. Vsesoyuz. Geogr. Ob-va **95**, No. 2, 134 (1963).

4. G. K. Rodgers, in *Proc. of the 11th Intern. Conf. on Great Lakes Res., Wisconsin, Apr. 18–20,* 1968, p. 942.

5. D. W. Hubbard and I. D. Spain, in *Proc. of the 16th Conf. on Great Lakes Research, Ann Arbor* (Michigan, 1973), p. 735.

6. M. A. Naumenko and S. G. Karetnikov, Meteorol. Gidrol., No. 4, 107 (1998).

7. A. I. Tikhomirov, *Thermal Conditions of Large Lakes* (Nauka, Leningrad, 1982) [in Russian].

8. S. S. Zilitinkevich and A. Yu. Terzhevik, Okeanologiya **27**, No. 5, 732 (1987).

9. S. S. Zilitinkevich, K. D. Kreiman, and A. Y. Terzhivik, J. Fluid Mech. **236**, 27 (1992).

10. J. Malm and L. Jonsson, Remote Sens. Environ. **48**, 332 (1994).

11. J. C. K. Huang, Geophys. Fluid Dyn. **3**, 1 (1972).

12. D. E. Farrow, J. Fluid Mech. **289**, 129 (1995).

13. D. E. Farrow, J. Fluid Mech. **303**, 279 (1995).

14. V. A. Kovalev and A. E. Ordanovich, *Physicomathematical Model of a Turbulent Horizontal Stratified Flow with Allowance for Coherent Structures. Pt. 1. Model Construction* (Dep. VINITI, Moscow, 1981), No. 2771-81 [in Russian].

15. N. S. Blokhina, A. V. Ovchinnikova, and A. E. Ordanovich, Vestn. Mosk. Un-ta, Fiz. Astron., No. 2, 60 (2002).

16. P. Roache, *Fundamentals of Computational Fluid Dynamics* (Hermosa Publ. Albuquerque, London, 1976; Mir, Moscow, 1980).